Supplementary Materials: Chemical Adsorption of HF, HCl, and H_2O onto YF_3 and Isostructural HoF_3 Surfaces by First Principles

Jennifer Anders, Henrik Wiedenhaupt, Beate Paulus

Contents

1. Computational Method Validation

1.1. Potential Files

We used the hard potential files for atoms available as recommended by VASP for very small bond distances, as e.g. the case for H−F, a central molecule of this study. We tested the effect of the hard potential files F_h and H_h vs. the normal ones F and H while keeping all other parameters, including the kinetic cutoff value constant as given in computational details. The first test system is the simple free, molecular HF in vacuum, which we need to calculate ΔE_{bond} of the adsorpted systems. When using the hard potential files, a bond distance of $R_{\text{H-F}} = 93.15$ pm is obtained. With the normal potential files, the bond elongates significantly by 0.62 pm. According to NIST, the experimental bond length is $R_{\text{H-F}} = 91.68$ pm [2] or by calculation e.g. 91.7 pm at the CCSD(T)/aug-cc-pVQZ level [1]. Consequently, the bond elongation equals a worse description.

We also tested the effect onto the surfaces by single point calculations with the normal potential files onto bare (100) and adsorbed (100)·HF isomer c (see Figure S5 **c**) built and relaxed at the hard potential file setup as described in the computational details. The adsorption energy obtained by applying the normal potential files is by -3.4 kJ·mol^{-1} or

4% stronger. Thus the normal vs. hard potential files also have a considerable effect on the adsorption energies.

1.2. Supercell Size

To ensure isolated adsorptions with non-interacting adsorbates, we tested supercell sizes ($n \times m \times p$) with $n, m, p = \{1 - 3\}$ UC onto the (010) surface with a single HF or H_2O molecule adsorbed. Note that each (010) UC corresponds to ($2 \times 1 \times 2$) YF_3-layers. The atomic positions of the adsorbate and the first YF_3-layer are relaxed. All other parameters equal those given within in the computational details for the isolated adsorption setup of the main paper.

Table S1. Scope of supercell size convergence onto the (010) YF_3 surface with a single adsorbate. Each column gives the supercell thickness in unit cell copies (UC) and YF_3-layers perpendicular to the surface. The supercells of 1 UC thickness are done for a single adsorbate of HF or H_2O:

YF_3·HF + YF_3·H_2O		YF_3·HF		YF_3·HF	
UC	layer	UC	layer	UC	layer
$1 \times 1 \times 1$	$2 \times 1 \times 2$	$1 \times 1 \times 2$	$2 \times 1 \times 4$	$1 \times 1 \times 3$	$2 \times 1 \times 6$
$2 \times 2 \times 1$	$4 \times 2 \times 2$	$2 \times 2 \times 2$	$4 \times 2 \times 4$	$2 \times 2 \times 3$	$4 \times 2 \times 6$
$2 \times 3 \times 1$	$4 \times 3 \times 2$	$2 \times 3 \times 2$	$4 \times 3 \times 4$	$2 \times 3 \times 3$	$4 \times 3 \times 6$
		$3 \times 3 \times 2$	$6 \times 3 \times 4$		

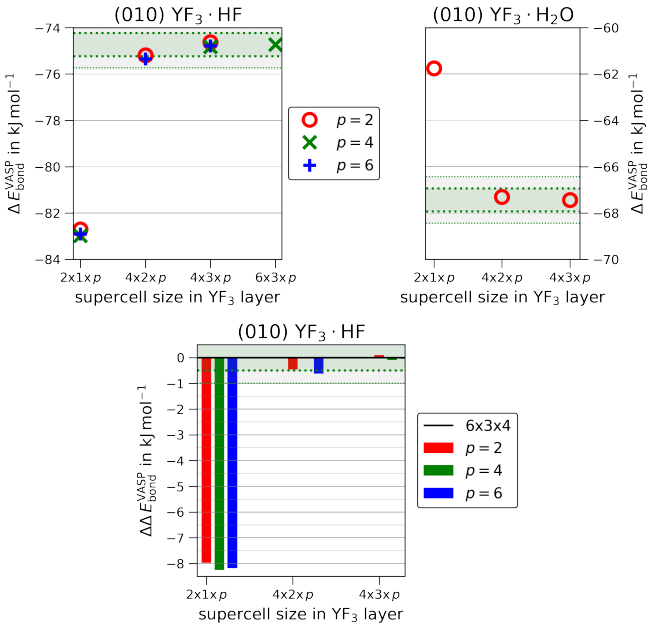

Figure S1. Supercell size convergence of ΔE_{bond} for the (010) YF_3 surface with a single adsorbate of HF (top left) or H_2O (top right). The x-axis gives the thickness perpendicular to the surface (p) in YF_3-layers. The difference to the biggest supercell ($\Delta E_{\text{bond}} - \Delta E_{\text{bond}}(6 \times 3 \times 4)$) is plotted for YF_3·HF (bottom). The green dotted lines and shaded areas visualize ± 1.0 and ± 0.5 kJ·mol^{-1}, respectively.

Comparing the two in-surface-plane lattice vectors, we find that the effect onto YF_3·H_2O is smaller than on YF_3·HF. Therefore, the bigger supercell tests were only done for the slower converging YF_3·HF. When increasing from the unit cell of (2x1) YF_3 layers to a (2x2) supercell of (4x2) YF_3 layers, the difference in ΔE_{bond} is as large as 7–8 kJ·mol^{-1}. A further increase to the square-like supercell of (4x3) YF_3 layers, only changes ΔE_{bond} by 0.5 kJ·mol^{-1}. The next possible supercell of (6x3) YF_3 layers alters the ΔE_{bond} by as little as 0.1 kJ·mol^{-1}. We thus consider a supercell size of ($2 \times 3 \times 2$) in UC or ($4 \times 3 \times 4$) in YF_3-layers as converged. This corresponds to almost square-like dimensions

of 12.6430 Å × 12.9900 Å × 13.6118 Å. The ΔE_{bond} differed by as little as 0.5 kJ·mol^{-1} compared to the largest tested supercell area of 18.9645 Å × 12.9900 Å × 13.6118 Å by (6 × 3 × 4) YF_3-layers. For the other surface cuts, supercells have been chosen that keep the dimensions similar.

Upon increasing the supercell thickness, the changes in relaxed adsorption energy ΔE_{bond} are very low. 2 YF_3-layers perpendicular to the surface give already a converged ΔE_{bond}. However, for the substoichiometric (101) surfaces, these were found to be unstable within the atomic position relaxations. Consequently, a thickness of 4 MF_3-layers is used for all supercells.

Table S2. Converged supercell sizes of all surface cuts with their corresponding surface area (A_{surf}), the total number of formula units ($N_{f.u.}$) and atoms within the supercell (N_{atoms}):

(*hkl*)	in UC	in layers	A_{surf} in Å^2	$N_{f.u.}$	N_{atoms}
(010)	(2 × 3 × 2)	(4 × 3 × 4)	(12.6430 × 12.9900)	48	192
(100)	(2 × 3 × 2)	(4 × 3 × 4)	(13.6117 × 12.9900)	48	192
(101)	(2 × 2 × 4)	(4 × 4 × 4)	(13.6117 × 15.3245)	64−8F	248
(011)	(2 × 2 × 4)	(4 × 4 × 4)	(12.6430 × 16.1330)	64	256

2. AIMD

An overview of all AIMD runtimes and temperatures is given in Table S3. Within the pure HF monolayers, the issue of infinite HF-chains forming by the periodic boundary conditions was frequently encountered due to the relatively small lattice vectors within the surface plane. These Ads-Ads interactions gave a more favorable energy than the interaction towards the surface. Accordingly, it was not helpful to judge adsorption events by the energy time series of the trajectory.

Table S3. Overview of AIMD simulation at different temperatures for pure monolayers of YF_3·$(Ads)_4$ and 1:1 mixed monolayers of YF_3·$(Ads_1)_4$·$(Ads_2)_4$ with summed up simulation times over all respective runs:

(*hkl*)	Ads	setup	T in K	runtime in ps
(010)	HF	a	50	1
	HF	a	100	2.5
	HF	a	200	25
	H_2O	a	50	1
	H_2O	a	100	2.5
	H_2O	a	200	25
	HF:H_2O 1:1	c	200	20
	HCl:H_2O 1:1	c	200	8
(011)	HF	b	50	1
	HF	b	100	2.5
	HF	b	200	25
	HF	b	300	1
	H_2O	b	50	1
	H_2O	b	100	2.5
	H_2O	b	200	25
	H_2O	b	300	1
(101)	HF	b	50	1
	HF	b	100	2.5
	HF	b	200	25
	HF	b	300	1
	H_2O	b	50	1
	H_2O	b	100	2.5
	H_2O	b	200	25

3. Structural Scope

This section visualizes all found 44 single adsorption conformations grouped form 60 relaxed structures for YF_3 and 58 for HoF_3 done in the isolated setup. All final electronic structure data used to calculate ΔE_{int} and ΔE_{bond} are available within the NOMAD repository (ID: xoipefEvRGOWfNVSx_R1MA).

Table S4. Structural Scope of MF_3·(Ads) giving the total number of different final conformers with the total number of all respective starting structures in parenthesis:

(*hkl*)	*n* Ads	YF_3	HoF_3
(010)	1 HF	5 (10)	5 (8)
	1 HCl	3 (6)	3 (6)
	1 H_2O	3 (7)	3 (7)
(100)	1 HF	4 (4)	4 (4)
	1 HCl	5 (5)	5 (5)
	1 H_2O	3 (4)	3 (3)
(011)	1 HF	3 (4)	3 (4)
	1 HCl	3 (4)	3 (4)
	1 H_2O	2 (3)	2 (3)
(101)	1 HF	5 (5)	5 (5)
	1 HCl	4 (4)	4 (5)
	1 H_2O	4 (4)	4 (4)

3.1. (010)

3.1.1. HF

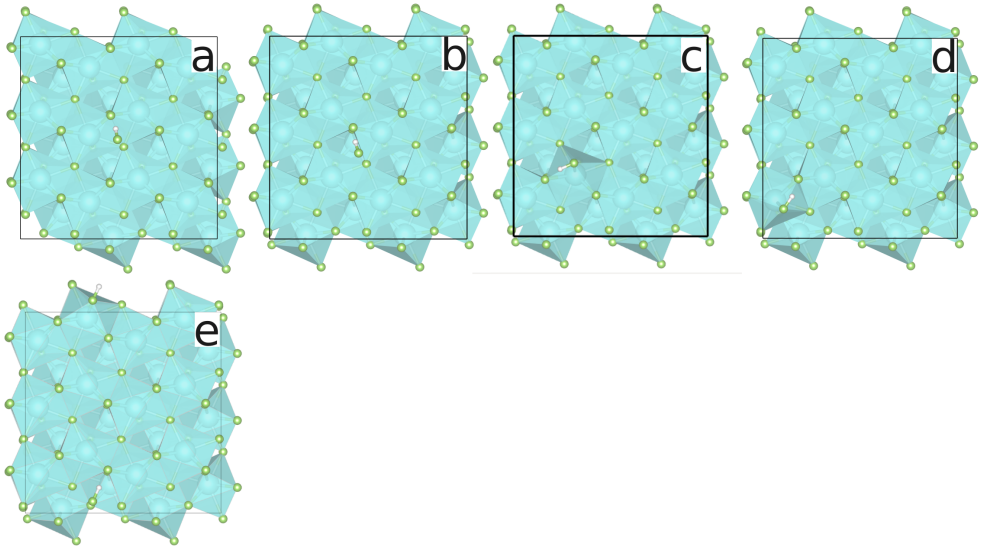

Figure S2. Relaxed adsorption structures of (010)·1HF in order of increasing $|\Delta E_{\text{bond}}|$ viewing onto the surface unit cell (black frame) made from ($2 \times 3 \times 2$) bulk unit cells. Two YF_3 structures were done for structural isomer **c** and five for structural isomer **e**. Three HoF_3 structures were done for structural isomer **c** and two for structural isomer **e**.

3.1.2. HCl

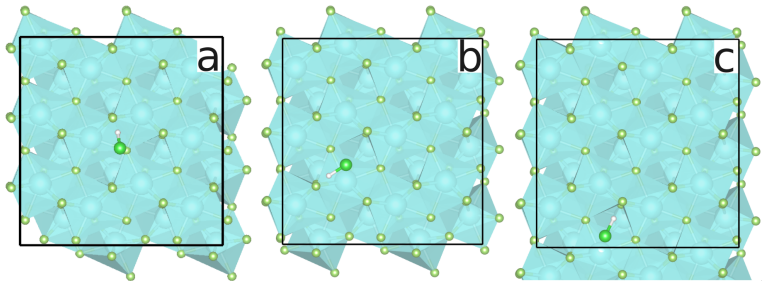

Figure S3. Relaxed adsorption structures of (010)·1HCl in order of increasing $|\Delta E_{\text{bond}}|$ viewing onto the surface unit cell (black frame) made from ($2 \times 3 \times 2$) bulk unit cells. Three structures were done for structural isomer **b** and two for structural isomer **c**.

3.1.3. H_2O

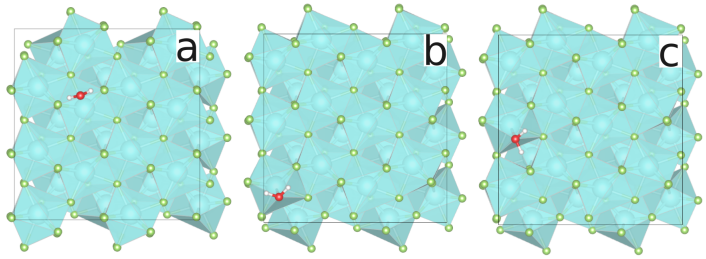

Figure S4. Relaxed adsorption structures of (010)·1H_2O in order of increasing $|\Delta E_{\text{bond}}|$ viewing onto the surface unit cell (black frame) made from ($2 \times 3 \times 2$) bulk unit cells. Three structures were done for structural isomer **b** and **c**.

3.2. (100)

3.2.1. HF

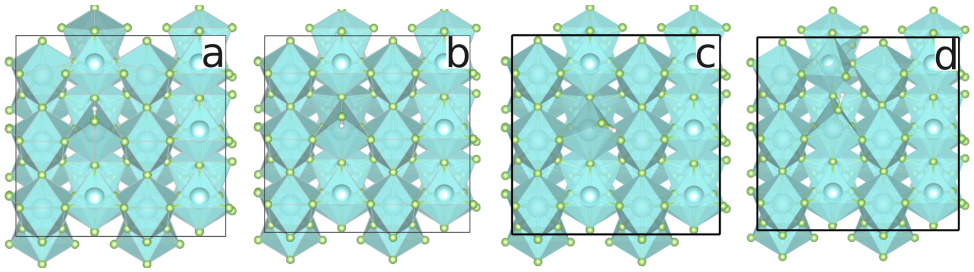

Figure S5. Relaxed adsorption structures of (100)·1HF in order of increasing $|\Delta E_{\text{bond}}|$ viewing onto the surface unit cell (black frame) made from ($2 \times 3 \times 2$) bulk unit cells.

3.2.2. HCl

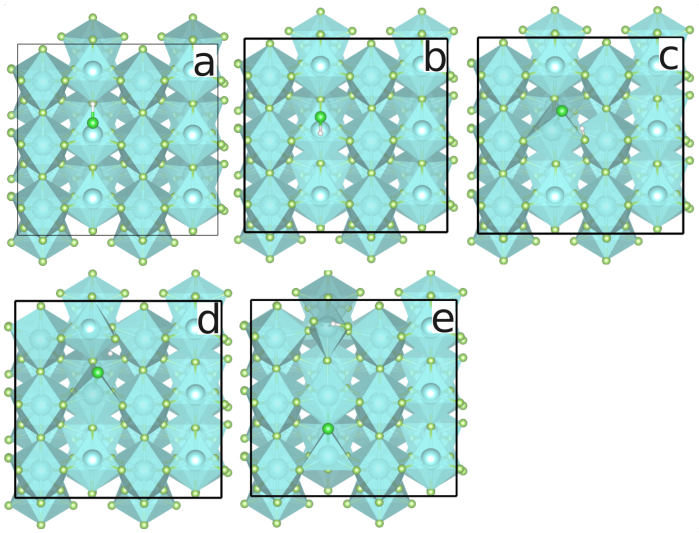

Figure S6. Relaxed adsorption structures of (100)·1HCl in order of increasing $|\Delta E_{\text{bond}}|$ viewing onto the surface unit cell (black frame) made from ($2 \times 3 \times 2$) bulk unit cells.

3.2.3. H_2O

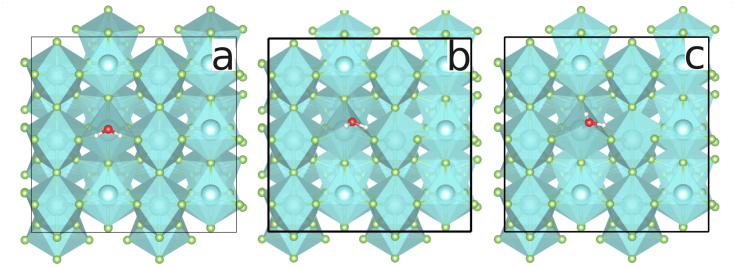

Figure S7. Relaxed adsorption structures of (100)·1H_2O in order of increasing $|\Delta E_{\text{bond}}|$ viewing onto the surface unit cell (black frame) made from ($2 \times 3 \times 2$) bulk unit cells. Two YF_3 structures were done for structural isomer **a**.

3.3. (011)

3.3.1. HF

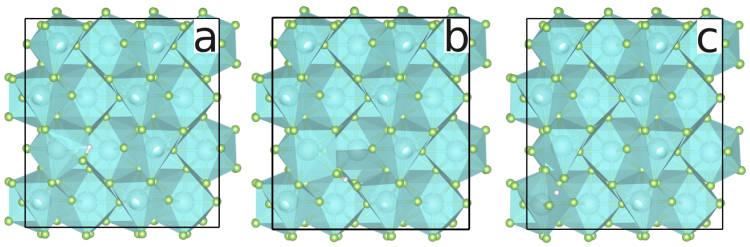

Figure S8. Relaxed adsorption structures of (011)·1HF in order of increasing $|\Delta E_{\text{bond}}|$ viewing onto the surface unit cell (black frame) made from ($2 \times 2 \times 4$) bulk unit cells. Two structures were done for structural isomer **c**.

3.3.2. HCl

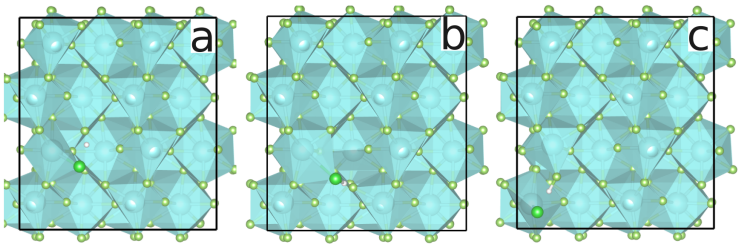

Figure S9. Relaxed adsorption structures of (011)·1HCl in order of increasing $|\Delta E_{\text{bond}}|$ viewing onto the surface unit cell (black frame) made from ($2 \times 2 \times 4$) bulk unit cells. Two structures were done for structural isomer **c**.

3.3.3. H_2O

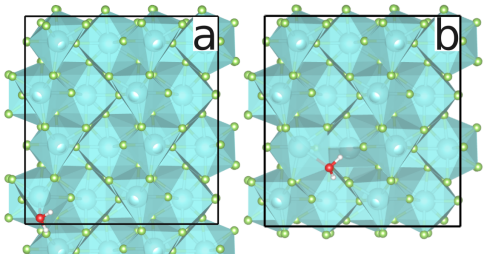

Figure S10. Relaxed adsorption structures of (011)·1H_2O in order of increasing $|\Delta E_{\text{bond}}|$ viewing onto the surface unit cell (black frame) made from ($2 \times 2 \times 4$) bulk unit cells. Two structures were done for structural isomer **b**.

3.4. (101)

3.4.1. HF

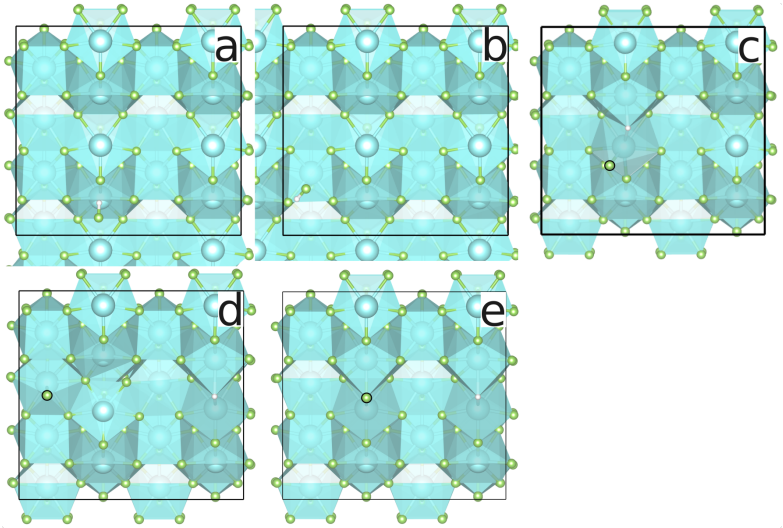

Figure S11. Relaxed adsorption structures of (101)·1HF in order of increasing $|\Delta E_{\text{bond}}|$ viewing onto the surface unit cell (black frame) made from ($2 \times 2 \times 4$) bulk unit cells. The hydride forming configurations **c**, **d** and **e** are called $MF_3{\cdot}H_{3\text{Å}}F$, $MF_3{\cdot}H_{3.5\text{Å}}F$ and $MF_3{\cdot}H_{7\text{Å}}F$ within the main paper according to the H−F distance.

3.4.2. HCl

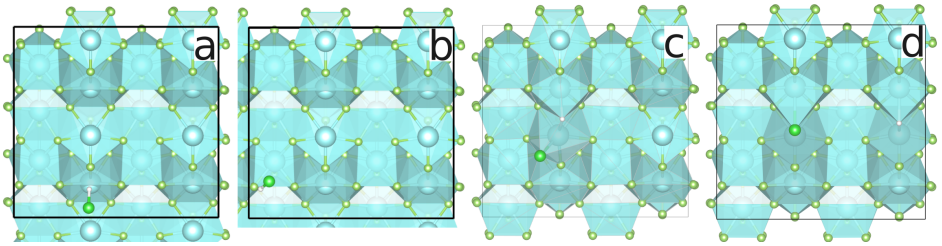

Figure S12. Relaxed adsorption structures of (101)·1HCl in order of increasing $|\Delta E_{\text{bond}}|$ viewing onto the surface unit cell (black frame) made from ($2 \times 2 \times 4$) bulk unit cells. The hydride forming configurations **c** and **d** are called $MF_3{\cdot}H_{3\text{Å}}Cl$ and $MF_3{\cdot}H_{7\text{Å}}Cl$ within the main paper according to the H−Cl distance. For configuration **d**, two structures were done for $HoF_3{\cdot}H_{7\text{Å}}Cl$.

3.4.3. H_2O

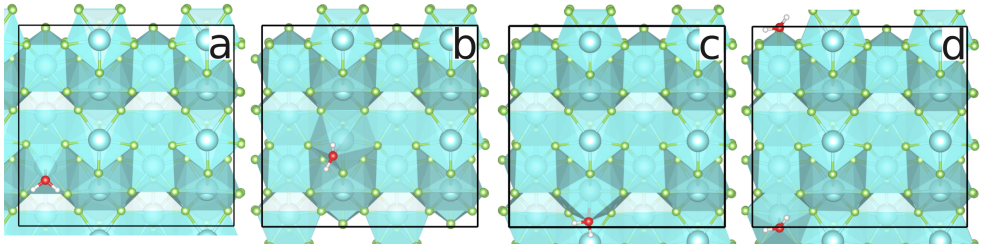

Figure S13. Relaxed adsorption structures of (101)·1H_2O in order of increasing $|\Delta E_{\text{bond}}|$ viewing onto the surface unit cell (black frame) made from ($2 \times 2 \times 4$) bulk unit cells.

4. Effect of Relaxation

Figures S14–S16 illustrate how the difference in adsorption energy between YF_3·Ads and HoF_3·Ads is affected by the relaxation energy of the reactants. $\Delta\Delta E_{\text{int}}^{\text{Y-Ho}}$ is defined analogously to $\Delta\Delta E_{\text{bond}}^{\text{Y-Ho}}$ (see Equation 5 of the main paper). The central, black diagonal plots $\Delta\Delta E_{\text{bond}}^{\text{Y-Ho}}$ against itself. A positive $\Delta\Delta E_{\text{int}}^{\text{Y-Ho}}$ (or $\Delta\Delta E_{\text{bond}}^{\text{Y-Ho}}$) means that the HoF_3·Ads is stronger bound than the respective YF_3·Ads. Therefore, values within the lower right triangle correspond to an increased difference between the two MF_3 upon reactant relaxation.

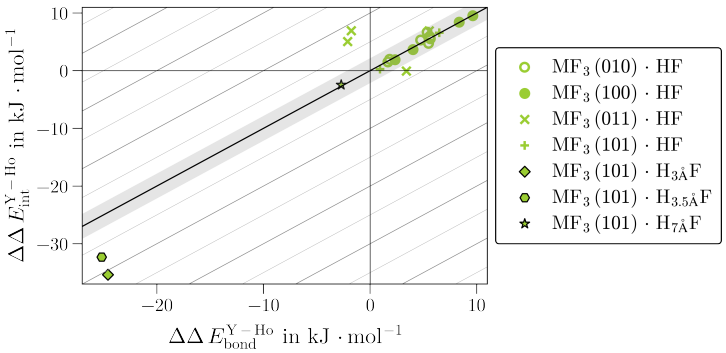

Figure S14. Difference of adsorption energies of YF_3·HF and HoF_3·HF with ($\Delta\Delta E_{\text{bond}}^{\text{Y-Ho}}$) or without ($\Delta\Delta E_{\text{int}}^{\text{Y-Ho}}$) relaxed reactants. An area of ± 2 kJ·mol^{-1} is shaded.

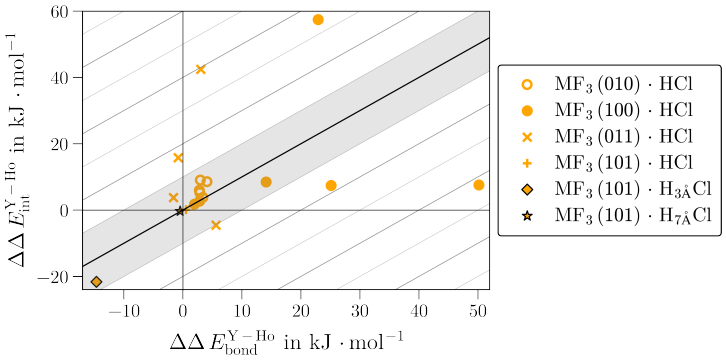

Figure S15. Difference of adsorption energies of YF_3·HCl and HoF_3·HCl with ($\Delta\Delta E_{\text{bond}}^{\text{Y-Ho}}$) or without ($\Delta\Delta E_{\text{int}}^{\text{Y-Ho}}$) relaxed reactants. An area of ± 10 kJ·mol^{-1} is shaded.

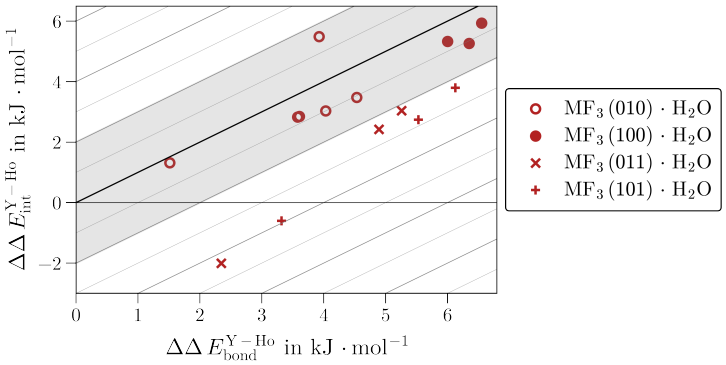

Figure S16. Difference of adsorption energies of YF_3·H_2O and HoF_3·H_2O with ($\Delta\Delta E_{\text{bond}}^{\text{Y-Ho}}$) or without ($\Delta\Delta E_{\text{int}}^{\text{Y-Ho}}$) relaxed reactants. An area of ± 2 kJ·mol^{-1} is shaded.

5. Averages over Structural Properties

The coordination of an adsorbate towards the surface has been considered a H-bond, if either the angle or distance satisfies at least the criteria of moderate H-bonds with $A_{\text{X-H}\cdots\text{F}_{\text{surf}}} \geq 130°$ or $R_{\text{H}\cdots\text{F}_{\text{surf}}} \leq 220$ pm [3].

For the structural properties (a) of bond distances and H-bond angle, its arithmetic mean and linearly weighted mean by ΔE_{bond} ($\overline{a}_E$) is given in Table S5 for each surface and over all surfaces. Note that the intra-adsorbate bond length ($R_{\text{O-H}}$) for MF_3·H_2O is given as the mean over both O−H bonds.

$$\overline{a}_E = \frac{\sum_i (-\Delta E_{\text{int},i}\, a_i)}{\sum_i (-\Delta E_{\text{bond},i})} \tag{1}$$

Table S5. Calculated means of intra-adsorbate bond length (R_{X-H}), H-bond angles ($A_{X-H\cdots F_{surf}}$) and distances ($R_{H\cdots F_{surf}}$), direct O/F/Cl to metal coordinations ($R_{X-Y/Ho_{surf}}$) without weight ($\overline{a}$) or weighted by ΔE_{bond} as given in Equation 1 ($\overline{a}_E$) for all non-hydride forming single adsorptions and without the 7 Å dissociated (100)·HCl structural isomer e; the $\overline{a}_E$ over all (*hkl*) are plotted in Figure 6 within the main paper:

			$\overline{R}_{X-H}$ / pm		$\overline{A}_{X-H\cdots F_{surf}}$ / °		$\overline{R}_{H\cdots F_{surf}}$ / pm		$\overline{R}_{X-Y/Ho_{surf}}$ / pm	
	(*hkl*)	MF_3	$\overline{a}$	$\overline{a}_E$	$\overline{a}$	$\overline{a}_E$	$\overline{a}$	$\overline{a}_E$	$\overline{a}$	$\overline{a}_E$
HF	(010)	Y	98	99	159	161	149	146	252	246
		Ho	98	98	156	157	152	149	244	244
	(100)	Y	100	103	159	162	130	130	241	237
		Ho	100	103	160	162	128	128	243	239
	(011)	Y	107	108	169	170	128	126	232	230
		Ho	107	108	169	170	128	126	235	234
	(101)	Y	95	96	151	148	165	165	260	260
		Ho	96	96	154	149	166	165	257	257
	all	Y	100	102	160	164	144	138	246	239
		Ho	100	103	160	162	144	137	242	239
HCl	(010)	Y	131	131	149	151	178	175	321	318
		Ho	132	133	153	155	166	164	310	308
	(100)	Y	149	163	155	156	107	107	289	277
		Ho	148	161	155	156	106	106	293	286
	(011)	Y	157	157	172	173	116	115	278	277
		Ho	158	158	172	173	114	113	279	278
	(101)	Y	130	130	156	154	188	189	—	—
		Ho	130	130	156	153	193	194	—	—
	all	Y	143	151	158	162	151	133	297	286
		Ho	143	152	159	162	147	129	295	288
H_2O	(010)	Y	98	98	155	156	182	173	262	248
		Ho	98	98	143	142	187	181	245	245
	(100)	Y	97	97	113	113	202	202	241	241
		Ho	97	97	114	114	203	203	244	244
	(011)	Y	98	98	141	142	195	195	241	241
		Ho	98	98	134	135	203	202	245	245
	(101)	Y	99	99	132	137	226	223	241	240
		Ho	98	99	143	144	233	226	244	243
	all	Y	98	98	138	138	198	197	249	243
		Ho	98	98	137	136	199	199	244	244

The non-/weighted averages of $\bar{R}_{X-H}$ hardly differ ($\leq$ 2 pm) between Y and Ho. Which MF_3·Ads possesses the smaller $\bar{R}_{X-H}$ is surface dependent. Only those H-bonds have been included that are either by distance ($\leq$ 220 pm) or by angle ($\geq$ 130°) at least within the moderate regime. By that criteria (101)·H_2O isomer a (see Figure S13 **a**) is just (hardly) included within YF_3 but (hardly) not in HoF_3.

The H-bond angles also hardly differ between the two metals for MF_3·HF, as well as MF_3·HCl with a maximum difference of 4°. Interestingly for adsorptions of H_2O, the weighted averages for (010) and (011)·H_2O are 14° and 7° wider for YF_3 than for HoF_3, while no such difference is observed for (100) and even the opposite for non-hydride forming (101)·H_2O. The $F-H\cdots F_{surf}$ distance is equivalent for YF_3 and HoF_3. For (010), however, the respective $Cl-H\cdots F_{surf}$ distance is significantly shorter in HoF_3. This is supported by the little bit wider H-bonds angles.

6. H-Bond Dissociated Structures

Adsorbates have been classified as H-bond dissociated if the distance within the adsorbate molecule is at least by 30 pm larger than the H-bond distance to a surface. This cutoff is illustrated in Figure S17 as dotted line.

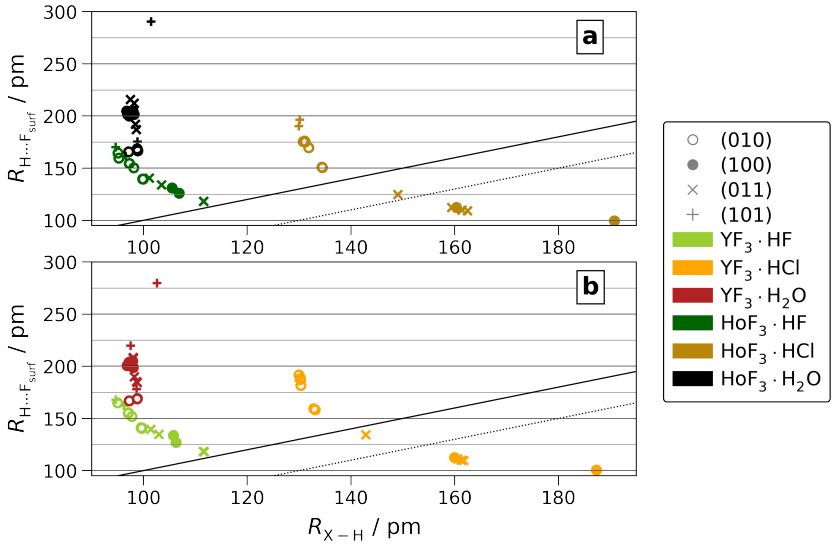

Figure S17. $R_{H\cdots F_{surf}}$ vs. R_{X-H} for HoF_3·Ads (**a**) and YF_3·Ads (**b**) for all non-hydride forming adsorptions but the 7 Å wide H-bond dissociated (100)·HCl. $R_{H\cdots F_{surf}} = R_{X-H} - \Delta R_x$ pm is highlight for $\Delta R_x = 0$ (solid line) and $\Delta R_x = 30$ (dotted line).

7. Hydride Forming Dissociated Structures

Figure S18 gives a version of Figure 6 **b** and **c** of the main paper including the hydride forming adsorptions of (101)·HF/HCl. Their negatively charged hydrogen forms no H-bond to F_{surf} but directly coordinates to M_{surf}. Thus, the distances of hydrogen towards the surface given in Figure S18 **a** are $R_{H\cdots M_{surf}}$ for the hydride forming adsorptions, while for any other, these are $R_{H\cdots F_{surf}}$, as in the main paper.

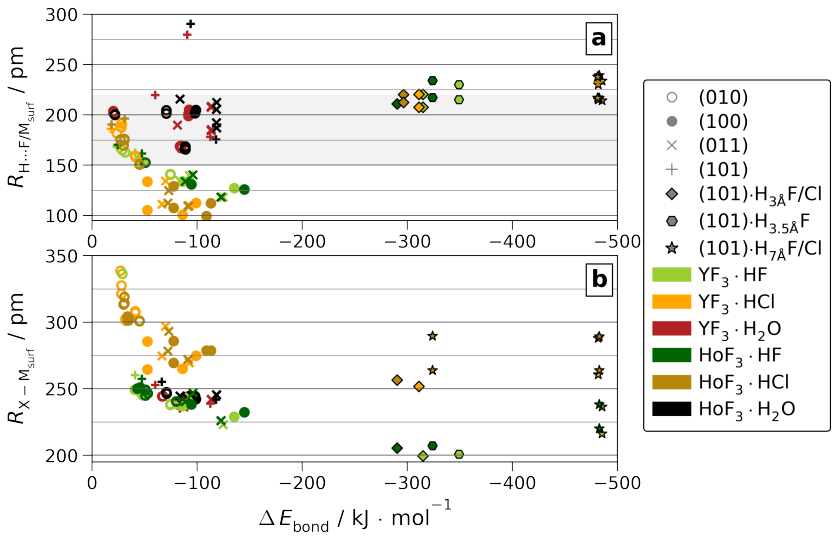

Figure S18. Coordination distances towards the surface by the adsorbate for H ($R_{H\cdots F/M_{surf}}$, **a**) and X = O/F/Cl ($R_{X-M_{surf}}$, **b**) vs. ΔE_{bond} for all single adsorptions.

Figure S19 gives the changes in partial Bader charges of $\geq$ 0.05 e upon adsorption for all metal centers. The partial charges of all F_{surf} remain unchanged compared to the bare surface. Upon hydride formation, the surface metal partial charges are increased by 0.4–0.5 e for each of the two M_{surf}(II) (next to) coordination sites for (101)·$H_{7Å}$F/Cl (and (101)·$H_{3.5Å}$F). In (101)·$H_{3Å}$F/Cl, with the halide and hydride coordinating to the same M_{surf}(II), again increased by 0.5 e, the remaining charge is split over two further M_{surf}(II).

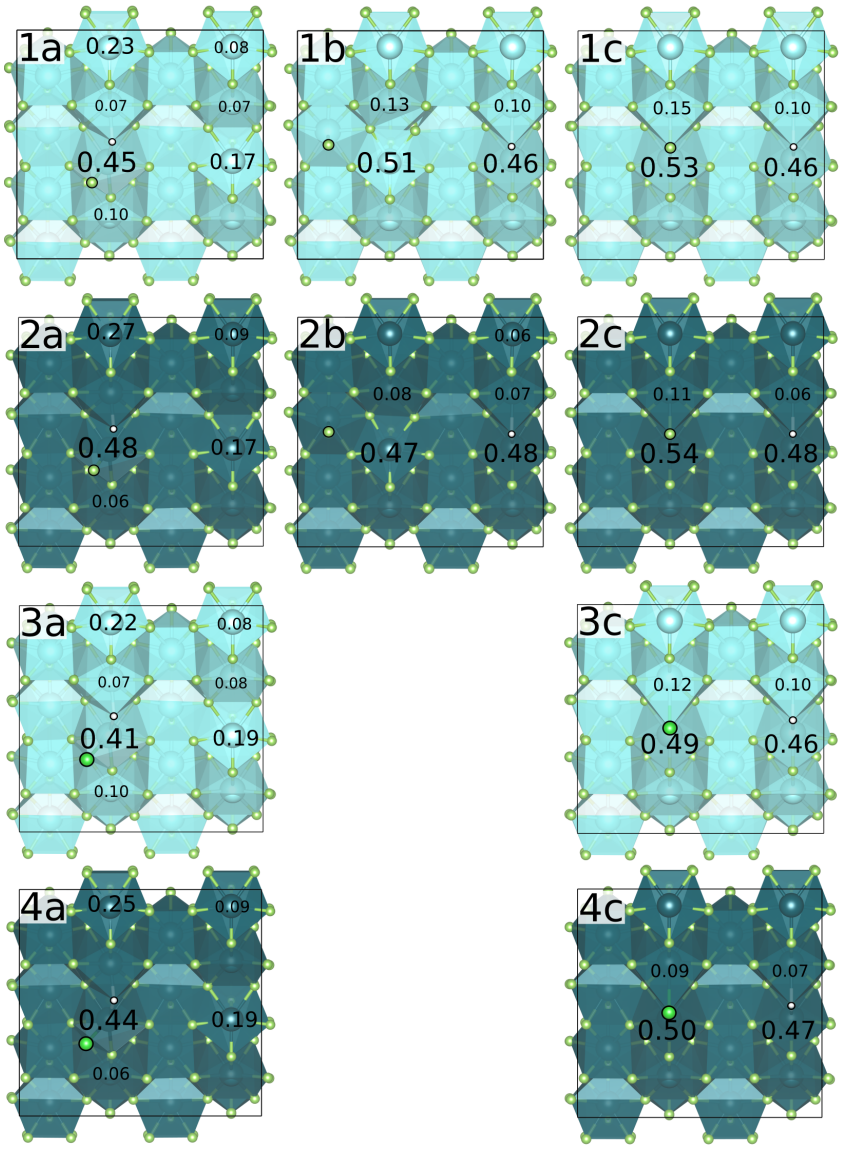

Figure S19. Changes in partial Bader charges ($\geq$ 0.05 e) of M_{surf} upon adsorbate dissociation for (101)·$H_{3Å}$F/Cl (**a**), (101)·$H_{3.5Å}$F (**b**) and (101)·$H_{7Å}$F/Cl (**c**) for YF_3·HF (**1a–1c**), HoF_3·HF (**2a–2c**), YF_3·HCl (**3a–3c**) and HoF_3·HCl (**4a–4c**).

8. Partial Charges

The partial charges of the adsorbed structure, as well as their differences compared to the free molecule are given in Figure S20–S23. See the main paper Figure 7 for the final partial charges of HF and HCl adsorptions.

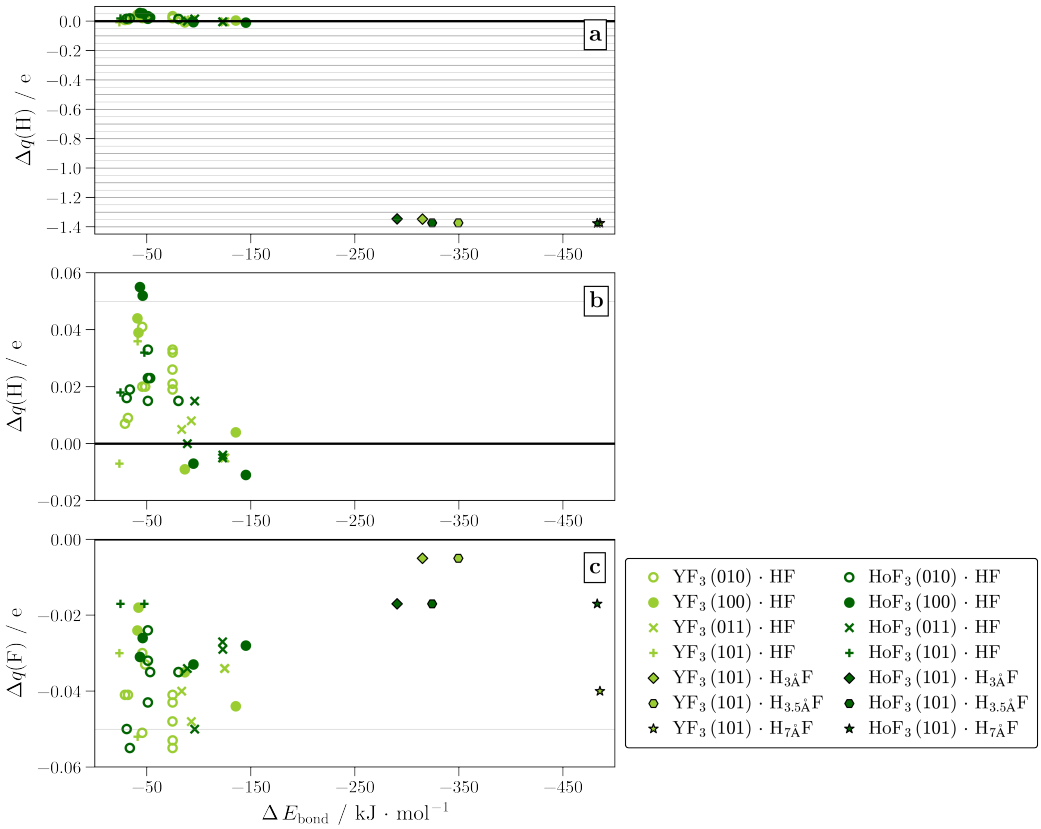

Figure S20. Change of partial Bader charges of HF adsorbed onto YF_3 or HoF_3 (Δq(H) **a** with zoom **b** and Δq(F) **c**) vs. molecular HF.

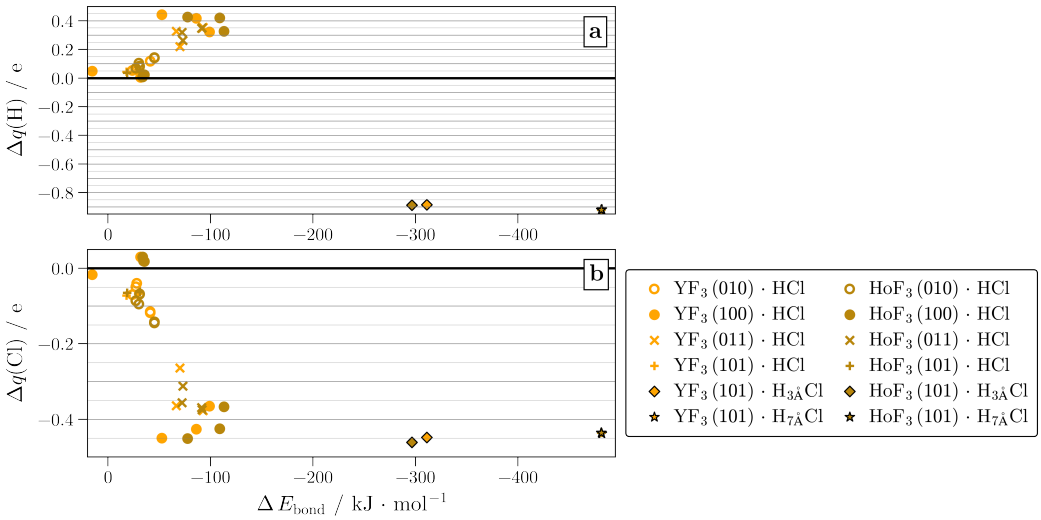

Figure S21. Change of partial Bader charges of HCl adsorbed onto YF_3 or HoF_3 (Δq(H) **a** and Δq(Cl) **b**) vs. molecular HCl.

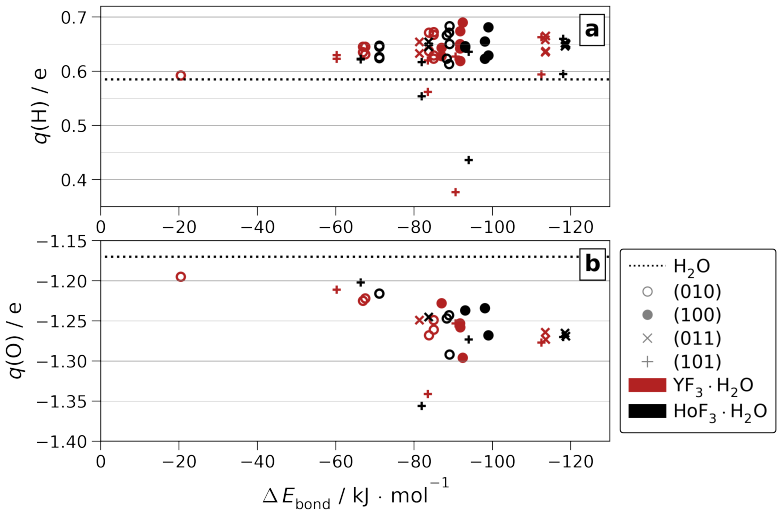

Figure S22. Partial Bader charges of molecular H_2O (dotted line) and adsorbed onto YF_3 or HoF_3 (q(H) **a** and q(O) **b**).

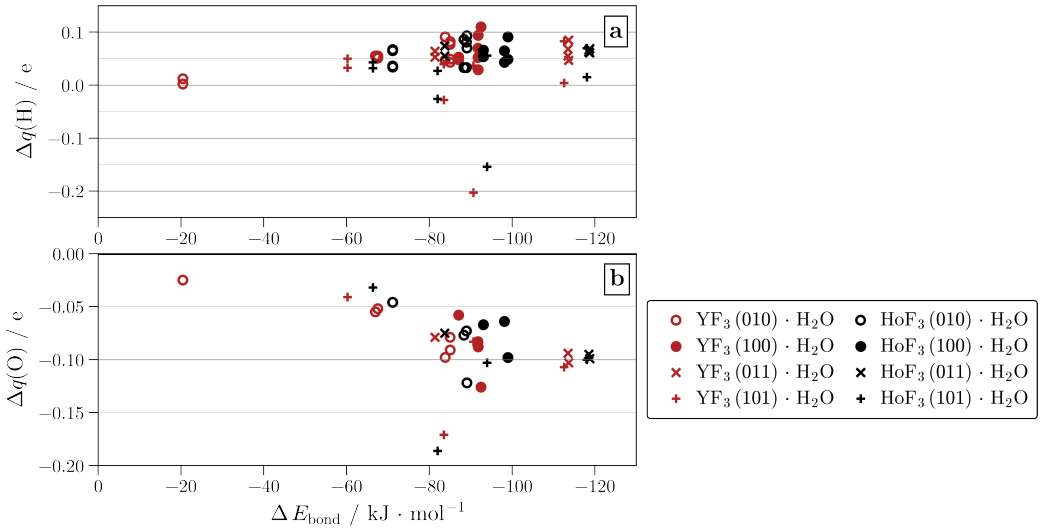

Figure S23. Change of partial Bader charges of H_2O adsorbed onto YF_3 or HoF_3 (Δq(H) **a** and Δq(O) **b**) vs. molecular H_2O.

9. Y vs. Ho Surface Dependence of Adsorption Energy

Figure S24 gives the difference in ΔE_{bond} between YF_3 and HoF_3 with the surface abundance ratios used to calculate the surface-weighted $\Delta\Delta E^{\text{Y-Ho}}_{\text{bond,\%}}$ of main paper Figure 8.

$$\Delta\Delta E^{\text{Y-Ho}}_{\text{bond}} = \Delta E^{\text{YF}_3\cdot\text{Ads}}_{\text{bond}} - \Delta E^{\text{HoF}_3\cdot\text{Ads}}_{\text{bond}} \quad (2)$$

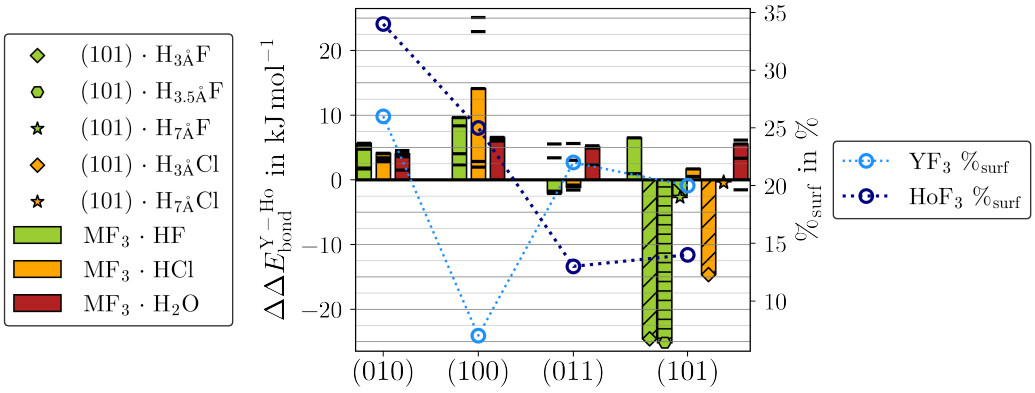

Figure S24. The difference in ΔE_{bond} between YF_3 and HoF_3 ($\Delta\Delta E_{\text{bond}}^{\text{Y-Ho}}$) (see Equation 2) is given for all single adsorptions (black lines). The bar plots highlight the respective strongest adsorbed structures. The hydride forming adsorptions of (101)·$H_{3Å}$F/Cl (upward stripes), (101)·$H_{3.5Å}$F (horizontal stripes) or (101)·$H_{7Å}$F/Cl (downward stripes) are given separately. The surface abundance ratios ($\%_{\text{surf}}$) for the ideal crystals are taken from [4].

References

1. NIST Computational Chemistry Comparison and Benchmark Database, NIST Standard Reference Database Number 101. 2022. Available online: http://cccbdb.nist.gov/ (accessed on 05 December 2022).
2. NIST Diatomic Spectral Database, NIST Standard Reference Database 114. Available online: https://doi.org/10.18434/T4T59X (accessed on 05 December 2022).
3. Jeffrey, G. *An Introduction to Hydrogen Bonding*; Oxford University Press: New York, NY, USA; Oxford, UK, 1997.
4. Anders, J.; Limberg, N.; Paulus, B. First Principle Surface Analysis of YF_3 and Isostructural HoF_3. *Materials* **2022**, *15*, 6048. https://doi.org/10.3390/ma15176048.